

# Propagation phenomena of fundamental torsional guided waves at axisymmetric defects

ねじり基本モードガイド波の軸対称欠陥における伝搬現象

Hideo Nishino<sup>1†</sup> and Hirofumi Saito<sup>1</sup> (<sup>1</sup>Institute of Tech. and Sci. Univ. of Tokushima)  
西野 秀郎<sup>1†</sup>, 斎藤浩史<sup>1</sup> (<sup>1</sup>徳島大 機械工)

## 1. Introduction

Investigations of reflection phenomena of the T(0,1) mode guided waves<sup>1)</sup> at gradually step-down axisymmetric defects were presented. A theoretical model<sup>2)</sup> calculating the reflection coefficients at the axisymmetric defect was introduced and was used for comparison to the experiments. It was confirmed that the frequency dependences of the reflection coefficients for the axisymmetric defects were in excellent agreements with the calculations.

## 2. Calculation model of reflection coefficient<sup>2)</sup>

Reflection and transmission phenomena of an ultrasonic guided wave are subject to the characteristic acoustic impedance  $Z = \rho v A$ , where  $A$  is the cross sectional area of the waveguide<sup>3)</sup>. Therefore, the reflection  $r_{12}$  and transmission  $t_{12}$  coefficients at a wall thinning are, respectively, described only with the cross sectional areas as follows:

$$r_{12} = (A_2 - A_1)/(A_2 + A_1), \quad t_{12} = 2A_2/(A_2 + A_1). \quad (1)$$

When the cross sectional area is changed gradually along the axial direction as shown in Fig. 1, the total reflection coefficient  $R$  can be described by integrating the reflection and transmission coefficients of the subdivided elements all through the entire region of the defect as follows:

$$R = \sum_{n=1}^N \left[ \prod_{m=1}^{n-1} (t_{m,m+1} t_{m+1,m}) r_{n,n+1} e^{i\{\text{or}-2(n-1)k\Delta z\}} \right] \quad (2)$$

where  $N$ ,  $\omega$ ,  $t$ ,  $k$  and  $\Delta z$  are number of subdivisions, frequency, time, wave number and axial length of subdivisions, respectively.

## 3. Example of calculation

Reflection coefficient of the defect (Fig.2;  $d_1=5.5\text{mm}$ ,  $d_2=2.75\text{mm}$ ) was obtained using eq. (2). Frequency and velocity of the T(0,1) mode were 70 kHz and 2850 m/s, respectively. 2-cycle Hanning-windowed signal was used. Figure 3 shows the time domain signal obtained. The two isolated wave packets were clearly confirmed. In accordance with eq. (2), the formation mechanism of the waveform is explained as follows (see Fig. 4): (a) Reflections occur in all the location of the tapered region. (b) The amplitude of each

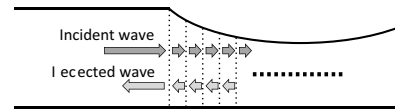


Fig. 1 Gradually step-down defect. Change of cross sectional area generates a reflected wave.

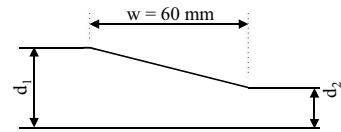


Fig. 2 Size of wall thinning of axisymmetric defect

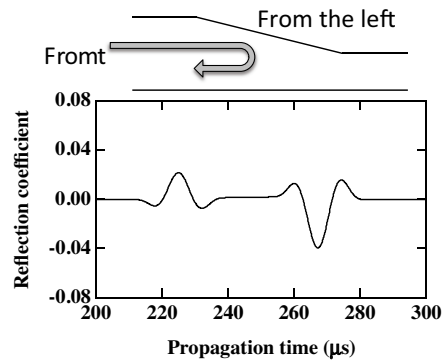


Fig. 3 Waveform reflected at the taper (calculated)

signal-element gradually increases with a decrease of the thickness, because the factor  $r_{n,n+1}$  of eqs. (2) and (1) takes larger value at thinner wall thickness. Furthermore, the amplitude at thinner end is two times larger than that at the thicker end. (c) Except the signal-elements generated near the thicker and thinner ends, the middle part of the signal-elements vanish because of the interference of the positive and negative signals. Eventually, the waveform observed can be obtained as shown in Fig. 4(c). Similar waveform obtained by the FEM calculation has been reported in the important precedent research<sup>4)</sup>.

## 4. Experimental verifications

Figure 5 shows the experimental apparatus. 60.5 mm outer diameter and 3.9 mm thick aluminum pipes were used. The piezoelectric ring-shaped sensor system having 16 transducer-elements were performed for generation and detection of the T(0,1) mode guided waves. 13-cycle Hanning-windowed signal was used. The center frequency  $f$  was varied from 24 kHz to 50

hidero.nishino@tokushima-u.ac.jp

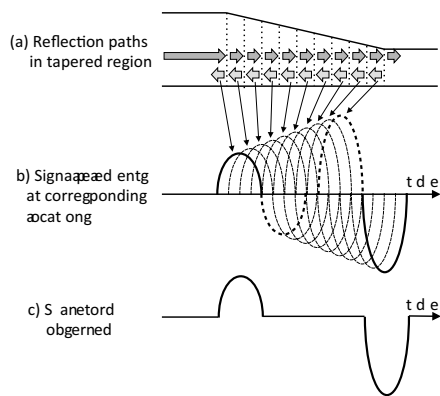


Fig. 4 Schematic illustration of the formation mechanism of the waveform

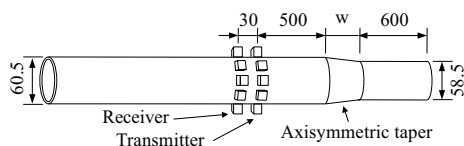


Fig. 5 Schematic illustration of the formation mechanism of the waveform

kHz with 2 kHz step. An axisymmetric tapered defect as shown in Fig. 2 ( $d_1=3.9\text{mm}$ ,  $d_2=1.9\text{mm}$ ) was introduced in the pipes. The width of the taper was set to be 45 and 60 mm.

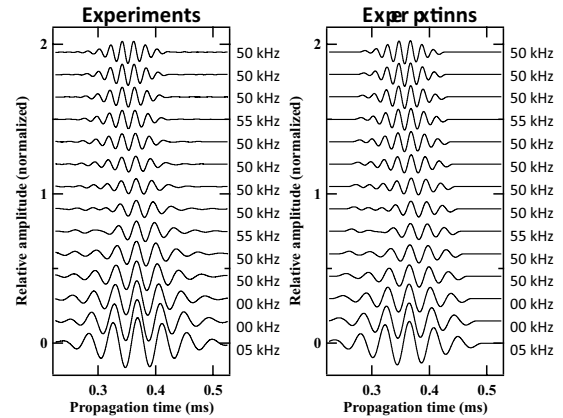
Figure 6 shows the frequency variations of the time domain signals of both the experimental and calculated results. The amplitudes observed were normalized by the input-signals. It was clearly confirmed that all the waveforms experimentally obtained agreed excellently with the corresponding calculation results. The reflection coefficients as a function of frequency were summarized in Fig. 7. The lines and circles indicate calculation and experimental results, respectively. As a matter of fact, all the calculation results are principally the same, when the horizontal axis is described as a function of the product of frequency and width,  $fw$ , of the taper instead of frequency.  $fw$  is added as the upper axis to each graph of Fig. 7.

## 5. Conclusion

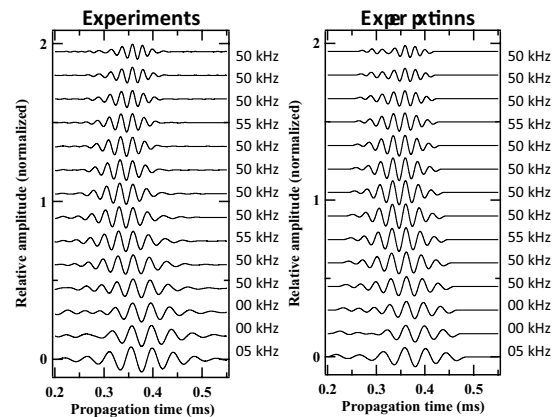
Reflection phenomena at the axisymmetric defects were investigated. The simple calculation model for obtaining the reflection coefficients was introduced and compared to the experimental results. It was confirmed that the calculations agreed excellently with the experiments. This paper revealed a mechanism of reflection phenomena at the axisymmetric defects.

## Acknowledgment

This work was supported by Nuclear and Industrial Safety Agency (NISA) of the Ministry of Economy, Trade and Industry (METI).



(a) taper width  $w = 45$  mm



(b) taper width  $w = 60$  mm

Fig. 6 Time domain signals of both obtained by the experiments and calculations

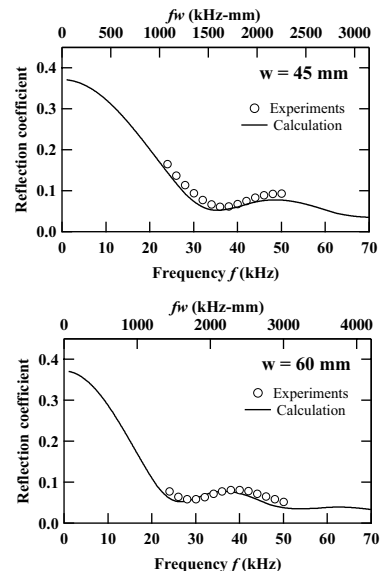


Fig. 7 Reflection coefficient vs. frequency. The calculations are the same, when the horizontal axis is described as a function of  $fw$ , instead of  $f$ .

## References

1. D. C. Gazis, JASA **31** (1959) 568.
2. Y. Nagashima et al, QNDE **28** (2009) 1583.
3. M. Choi et al, UFFC **51** (2004) 640.
4. R. Carandente et al, JASA **127** (2010) 3440.